
Learning to Approximate a Bregman Divergence: Supplementary Material

Anonymous Author(s)

Affiliation

Address

email

1 Appendix

2 In this appendix, we provide several additional results:

- 3 • Background mathematical concepts required for the proofs (A1)
- 4 • Proof of the approximation bound (A2)
- 5 • Proof of the Rademacher complexity bound (A3)
- 6 • Proof of the metric learning generalization error bound (A4)
- 7 • Discussion of the regression setting, including generalization error (A5)
- 8 • Discussion of the case where $K < n$ (A6)
- 9 • Some additional details omitted from the discussion of the algorithms (A7)
- 10 • Additional experimental results, including results on regression and classification (A8)

11 A1 Covering number

12 This is a brief overview of covering numbers from [1]. Let $(\Omega, \|\cdot\|)$ be a metric space and $\Omega \subset \mathbb{U}$.
13 For any $\epsilon > 0$, $\mathbb{X}_\epsilon \subset \mathbb{U}$ is an ϵ -covering of Ω if:

$$\min_{\hat{\mathbf{x}} \in \mathbb{X}_\epsilon} \|\mathbf{x} - \hat{\mathbf{x}}\| \leq \epsilon \quad \forall \mathbf{x} \in \Omega.$$

14 The covering number $\mathcal{N}(\Omega, \epsilon, \|\cdot\|)$ is defined as the minimum cardinality of an ϵ -covering of Ω . By
15 volumetric arguments, the covering number of the norm ball of radius R in d -dimension $\mathcal{B}(R)$ is
16 bounded as below:

$$\left(\frac{R}{\epsilon}\right)^d \leq \mathcal{N}(\mathcal{B}(R), \epsilon, \|\cdot\|) \leq \left(\frac{2R}{\epsilon} + 1\right)^d.$$

17 In this paper we only consider the $\|\cdot\|_\infty$ on the input space. We construct a covering set by dividing
18 the space into hyper-cubes of side length 2ϵ as depicted in Figure 1. This construction provides us a
19 covering set of size $\mathcal{N}(\mathcal{B}(R), \epsilon, \|\cdot\|_\infty) \leq \lceil R/\epsilon \rceil^d$.

20 A2 Approximation Guarantees

21 Before proceeding with the proof we state a useful lemma.

22 **Lemma 1.** [6] For any two vectors $\mathbf{r}_1, \mathbf{r}_2 \in \mathbb{R}^d$,

23

$$\sup_{\|\mathbf{u}\|_\infty \leq \rho} \langle \mathbf{r}_1 - \mathbf{r}_2, \mathbf{u} \rangle \leq \delta \iff \|\mathbf{r}_1 - \mathbf{r}_2\|_1 \leq \delta/\rho.$$

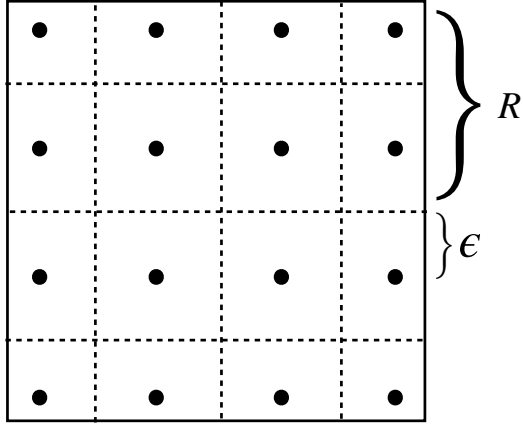


Figure 1: Sketch of a 2-dimensional hyper-cube of radius R , covered by ∞ -norm balls of radius ϵ .

24 **Proof of Theorem 1.**

25 Let $\mathbb{X}_\epsilon = \{\hat{\mathbf{x}}_1, \dots, \hat{\mathbf{x}}_K\}$ be an ϵ -cover for $\mathcal{B}(R)$ as constructed in A1. We have:

$$\epsilon = \frac{R}{\lfloor K^{1/d} \rfloor} \leq 2RK^{-1/d}.$$

26 Let $\hat{\mathbf{x}} = \arg \min_{\hat{\mathbf{x}}_i \in \mathbb{X}_\epsilon} \|\mathbf{x} - \hat{\mathbf{x}}_i\|_\infty$. We know $\|\mathbf{x} - \hat{\mathbf{x}}\|_\infty \leq \epsilon$ due to construction of \mathbb{X}_ϵ . Consider
 27 the piecewise linear function, $h : \mathbb{R}^d \rightarrow \mathbb{R}$, defined as follows:

$$h(\mathbf{x}) \triangleq \max_i \phi(\hat{\mathbf{x}}_i) + \langle \nabla \phi(\hat{\mathbf{x}}_i), \mathbf{x} - \hat{\mathbf{x}}_i \rangle. \quad (1)$$

28 We have:

$$\begin{aligned} 0 &\leq \phi(\mathbf{x}) - h(\mathbf{x}) \\ &\leq \phi(\mathbf{x}) - \phi(\hat{\mathbf{x}}) - \langle \nabla \phi(\hat{\mathbf{x}}), \mathbf{x} - \hat{\mathbf{x}} \rangle \\ &\leq \langle \nabla \phi(\mathbf{x}) - \nabla \phi(\hat{\mathbf{x}}), \mathbf{x} - \hat{\mathbf{x}} \rangle \\ &\leq \|\nabla \phi(\mathbf{x}) - \nabla \phi(\hat{\mathbf{x}})\|_1 \|\mathbf{x} - \hat{\mathbf{x}}\|_\infty \\ &\leq \beta \|\mathbf{x} - \hat{\mathbf{x}}\|_\infty^2 \leq \beta \epsilon^2 = 4\beta R^2 K^{-2/d}. \end{aligned}$$

29 Therefore (9) in the main paper is shown. For proving (10) consider covering points $\hat{\mathbf{x}}_i$ in a δ -ball
 30 around \mathbf{x} .

$$\begin{aligned} &\langle \nabla \phi(\mathbf{x}) - \nabla h(\mathbf{x}), \mathbf{x} - \hat{\mathbf{x}}_i \rangle \\ &= \langle \nabla \phi(\mathbf{x}) - \nabla \phi(\hat{\mathbf{x}}_i), \mathbf{x} - \hat{\mathbf{x}}_i \rangle \\ &+ \phi(\hat{\mathbf{x}}_i) + \langle \nabla \phi(\hat{\mathbf{x}}_i), \mathbf{x} - \hat{\mathbf{x}}_i \rangle \quad * (\langle h(\mathbf{x}) \rangle) \\ &- h(\hat{\mathbf{x}}_i) - \langle \nabla h(\mathbf{x}), \mathbf{x} - \hat{\mathbf{x}}_i \rangle \quad ** (\langle -h(\mathbf{x}) \rangle) \\ &\leq \|\nabla \phi(\mathbf{x}) - \nabla \phi(\hat{\mathbf{x}}_i)\|_1 \|\mathbf{x} - \hat{\mathbf{x}}_i\|_\infty \\ &\leq \beta \|\mathbf{x} - \hat{\mathbf{x}}_i\|_\infty^2 \leq \beta \delta^2. \end{aligned} \quad (2)$$

31 * is true due to the way $h(\mathbf{x})$ is defined in (1). ** is true due to convexity. By a convex combination
 32 of inequalities in (2) we get:

$$\langle \nabla \phi(\mathbf{x}) - \nabla h(\mathbf{x}), \mathbf{x} - \sum_i \alpha_i \hat{\mathbf{x}}_i \rangle \leq \beta \delta^2. \quad (3)$$

33 Next we will prove $\mathbf{x} - \sum_i \alpha_i \hat{\mathbf{x}}_i$ can represent any vector \mathbf{r} of size $\|\mathbf{r}\|_\infty \leq \delta - 2\epsilon$. From there by
 34 using Lemma 1 and choosing $\delta = 4\epsilon$ we'll get

$$\|\nabla \phi(\mathbf{x}) - \nabla h(\mathbf{x})\|_1 \leq \beta \delta^2 / (\delta - 2\epsilon) \leq 16\beta R^2 K^{-1/d}.$$

35 If $\delta \geq 2\epsilon$ and \mathbf{x} is no closer than δ to the boundaries of $\mathcal{B}(R)$, we can consider hyper-cubes $\mathcal{B}(\epsilon)$
 36 fitted to each corner of $\mathcal{B}(\delta)$ centered at \mathbf{x} as in the 2-dimensional case depicted by Figure 2. There
 37 has to be covering points in each of these ϵ -hyper-cubes, otherwise their center is further away from
 38 all covering points by more than ϵ . As depicted by Figure 2 the convex hull of such covering points
 39 includes a $(\delta - 2\epsilon)$ -hyper-cube centered at \mathbf{x} . Therefore any vector of size $(\delta - 2\epsilon)$ can be represented
 by $(\mathbf{x} - \sum_i \alpha_i \hat{\mathbf{x}}_i)$.

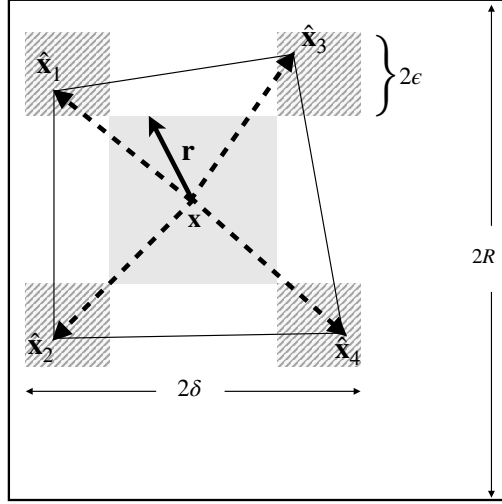


Figure 2: The 2-dimensional sketch of the input space $\mathcal{B}(R)$ along with $\mathcal{B}(\delta)$ centered at \mathbf{x} . Four dashed vectors represent $\mathbf{x} - \hat{\mathbf{x}}_k$. Using a convex combination of these vectors we can represent any vector \mathbf{r} (solid vector) of size $\|\mathbf{r}\|_\infty = \delta - 2\epsilon$.

40

41 The proof of (11) in the main paper is done by combining the approximation error of the gradient and
 42 the convex function as follows:

$$\begin{aligned}
 D_\phi(\mathbf{x}, \mathbf{x}') - D_h(\mathbf{x}, \mathbf{x}') &= \phi(\mathbf{x}) - \phi(\mathbf{x}') - \langle \nabla \phi(\mathbf{x}'), \mathbf{x} - \mathbf{x}' \rangle \\
 &\quad - h(\mathbf{x}) + h(\mathbf{x}') + \langle \nabla h(\mathbf{x}'), \mathbf{x} - \mathbf{x}' \rangle \\
 &\leq \phi(\mathbf{x}) - h(\mathbf{x}) \\
 &\quad + \langle \nabla h(\mathbf{x}') - \nabla \phi(\mathbf{x}'), \mathbf{x} - \mathbf{x}' \rangle \\
 &\leq |\phi(\mathbf{x}) - h(\mathbf{x})| \\
 &\quad + \|\nabla \phi(\mathbf{x}) - \nabla h(\mathbf{x})\|_1 \|\mathbf{x} - \mathbf{x}'\|_\infty \\
 &\leq 36\beta R^2 K^{-1/d}.
 \end{aligned}$$

43 The other side of the inequality can be shown similarly.

44 A3 Rademacher complexity of piecewise linear Bregman divergences

45 The Rademacher complexity $R_m(\mathcal{F})$ of a function class \mathcal{F} is defined as the expected maximum
 46 correlation of a function class with binary noise. Bounding the Rademacher complexity of a function
 47 class provides us with a measure of how complex the class is. This measure is used in computing
 48 probably approximately correct (PAC) bounds for learning tasks such as classification, regression,
 49 and ranking. Let

$$\mathcal{F}_{P,L} \triangleq \{h : \mathbb{R}^d \rightarrow \mathbb{R} \mid h(\mathbf{x}) = \max_{k \in [K]} \mathbf{a}_k^T \mathbf{x} + b_k, \|\mathbf{a}_k\|_1 \leq L\}$$

50 be the class of L -Lipschitz max-affine functions. Also let

$$\mathcal{D}_{P,L} \triangleq \{h(\mathbf{x}) - h(\mathbf{x}') - \nabla h(\mathbf{x}')^T (\mathbf{x} - \mathbf{x}') \mid h \in \mathcal{F}_{P,L}\}$$

51 be the class of Bregman divergences parameterized by a max-affine functions.

52

53 **Lemma 2.** *The Radamacher complexity of Bregman divergences parameterized by a max-affine*
 54 *function $R_m(\mathcal{D}_{P,L}) \leq 4KLR\sqrt{(2\ln(2d+2))/m}$.*

55 Proof. Define: $p(\mathbf{x}) \triangleq \arg \max_k \mathbf{a}_k^T \mathbf{x} + b_k$

$$\begin{aligned} \mathcal{D}_{P,L} &= \{h(\mathbf{x}) - h(\mathbf{x}') - \nabla h(\mathbf{x}')^T (\mathbf{x} - \mathbf{x}') \mid h \in \mathcal{F}_{P,L}\} \\ &= \{\mathbf{a}_{p(\mathbf{x})}^T \mathbf{x} + b_{p(\mathbf{x})} - \mathbf{a}_{p(\mathbf{x}')}^T \mathbf{x} - b_{p(\mathbf{x}')} \mid \|\mathbf{a}_i\|_1 \leq L\} \\ &= \{\mathbf{a}_{p(\mathbf{x})}^T \mathbf{x} + c_{p(\mathbf{x})} - \mathbf{a}_{p(\mathbf{x}')}^T \mathbf{x} - c_{p(\mathbf{x}')} \\ &\quad \mid \|\mathbf{a}_i\|_1 \leq L, c_i = b_i - b_{p(0)} + LR\}. \end{aligned}$$

56 Note that $|c_i| \leq LR$:

$$-c_i = b_{p(0)} - b_i - LR = \max_k b_k - b_i - LR \geq -LR.$$

57 For the other side, consider \mathbf{x} such that $h(\mathbf{x}) = \mathbf{a}_i^T \mathbf{x} + b_i$. If no such \mathbf{x} exists, we can discard the i^{th}
 58 hyper-plane. Therefore:

$$\begin{aligned} -c_i &= b_{p(0)} - b_i - LR = \max_k b_k - b_i - LR \\ &= h(0) - h(\mathbf{x}) + \mathbf{a}_i^T \mathbf{x} - LR \\ &\leq L\|0 - \mathbf{x}\|_\infty + \|\mathbf{a}_i\|_1 \|\mathbf{x}\|_\infty - LR \leq LR. \end{aligned}$$

59 Now we are ready to compute the Radamacher complexity:

$$\begin{aligned} R_m(\mathcal{D}_{P,L}) &= \frac{1}{m} \mathbb{E}_\sigma \sup \sum_{i=1}^m \sigma_i D_h(\mathbf{x}_i, \mathbf{x}'_i) \\ &= \frac{1}{m} \mathbb{E}_\sigma \sup_{\substack{\forall k \|\mathbf{a}_k\|_1 \leq L \\ \forall k \|c_k\|_1 \leq LR}} \sum_{i=1}^m \sigma_i (\mathbf{a}_{p(\mathbf{x}_i)}^T \mathbf{x}_i + c_{p(\mathbf{x}_i)} \\ &\quad - \mathbf{a}_{p(\mathbf{x}'_i)}^T \mathbf{x}'_i - c_{p(\mathbf{x}'_i)}) \\ &\leq \frac{2}{m} \mathbb{E}_\sigma \sup_{\substack{\forall k \|\mathbf{a}_k\|_1 \leq L \\ \forall k \|c_k\|_1 \leq LR}} \sum_{i=1}^m \sum_{k=1}^K |\sigma_i (\mathbf{a}_k^T \mathbf{x}_i + c_k)| \\ &= \frac{2K}{m} \mathbb{E}_\sigma \sup_{\substack{\|\mathbf{a}_1\|_1 \leq L \\ \|c_1\|_1 \leq LR}} \sum_{i=1}^m \left| \sigma_i \begin{bmatrix} c_1/R \\ \mathbf{a}_1 \end{bmatrix}^T \begin{bmatrix} R \\ \mathbf{x}_i \end{bmatrix} \right|. \end{aligned}$$

60 The last expression is $2K$ times the complexity of a Lipschitz linear function which is computed in
 61 [9], Sec. 26.2. Therefore:

$$\begin{aligned} R_m(\mathcal{D}_{P,L}) &\leq 2K \left\| \begin{bmatrix} c_1/R \\ \mathbf{a}_1 \end{bmatrix} \right\|_1 \\ &\quad \times \sup_i \left\| \begin{bmatrix} R \\ \mathbf{x}_i \end{bmatrix} \right\|_\infty \sqrt{(2\ln(2d+2))/m} \\ &\leq 2K \times 2L \times R \times \sqrt{(2\ln(2d+2))/m}. \end{aligned}$$

62

63 A4 PAC bounds for piecewise Bregman divergence metric learning

64 In this section we use the Rademacher complexity bounds derived in section A3 along with ap-
 65 proximation guarantees of section A2 to provide standard generalization bounds for empirical risk
 66 minimization under our divergence learning framework.

67 Proof of Theorem 2

68 The proof is very similar to that of Radamacher complexity bounds for soft-SVM given in [9]. First
 69 from Theorem 26.12 in [9] for a ρ -Lipschitz loss function $L(f, z) \leq M$ with probability of at least
 70 $1 - \delta$ we have for all $f \in \mathcal{F}$:

$$L_\mu(f) \leq L_{S_m}(f) + 2\rho R_m(\mathcal{F}) + M\sqrt{(2\ln(2/\delta))/m}.$$

71 Now note that the hinge loss is 1-Lipschitz, bounded by 1. By substituting $\mathcal{F} = \mathcal{D}_{P,L}$, $f = h_m$ and
 72 $L = L^{hinge}$ we get:

$$L_{\mu}^{hinge}(D_{h_m}) \leq L_{S_m}^{hinge}(D_{h_m}) + 4R_m(\mathcal{D}_{P,L}) + \sqrt{(2 \ln(2/\delta))/m} \quad w.p. \geq 1 - \delta. \quad (4)$$

73 Since we are also learning the Lipschitz constant L , for having a generalization bound we should
 74 express a uniform result for all L . We use the trick used in [9] for providing the union bound. To
 75 proceed for any integer i take $L_i = 2^i$ and take $\delta_i = \delta/(2i^2)$. Using (4) we have for any $L \leq L_i$,

$$L_{\mu}^{hinge}(D_{h_m}) \leq L_{S_m}^{hinge}(D_{h_m}) + 4R_m(\mathcal{D}_{P,L}) + \sqrt{(2 \ln(2/\delta_i))/m} \quad w.p. \geq 1 - \delta_i.$$

76 Applying the union bound and noting $\sum_{i=1}^{\infty} \delta_i \leq \delta$ this holds for all i with probability at least $1 - \delta$.
 77 Now take $i = \lceil \log_2 L \rceil \leq \log_2 L + 1$ then $\frac{2}{\delta_i} = \frac{(2i)^2}{\delta} \leq \frac{4 \log_2 L}{\delta}$. Therefore:

$$L_{\mu}^{hinge}(D_{h_m}) \leq L_{S_m}^{hinge}(D_{h_m}) + 4R_m(\mathcal{D}_{P,L}) + (\sqrt{4 \ln(4 \log_2 L) + \ln(1/\delta)})/\sqrt{m},$$

78 with probability at least $1 - \delta$.

79 A5 Regression Setting

80 Next we consider the regression scenario, and discuss generalization bounds. Here we are interested
 81 in the expected squared loss between the Bregman divergence obtained from the minimizer of the
 82 regression loss (5) and the true divergence value, on unseen (test) data.

83 Suppose the function ℓ_t consists of a pair of points from X , say \mathbf{x}_{i_t} and \mathbf{x}_{j_t} , and the y_t value is a
 84 noisy version of the the target (ground truth) Bregman divergence between \mathbf{x}_{i_t} and \mathbf{x}_{j_t} . A standard
 85 least squares loss function (with no regularization) would seek to solve

$$\min_{\phi \in \mathcal{F}} \sum_{t=1}^m (D_{\phi}(\mathbf{x}_{i_t}, \mathbf{x}_{j_t}) - y_t)^2.$$

86

87 Suppose we observe the data $S_m = \{(\mathbf{x}_{i_t}, \mathbf{x}_{j_t}, y_t) | t \in [m]\}$, where $\mathbf{x} \in \mathbb{R}^d$ and $y \in \mathbb{R}$. We will
 88 model the response random variable y as a Bregman divergence $D_h(\mathbf{x}_i, \mathbf{x}_j)$ with $h \in \mathcal{F}_{P,L}$. Let
 89 $h_m : \mathbb{R}^d \rightarrow \mathbb{R}$ be the empirical risk minimizer of

$$\min_{h \in \mathcal{F}_{P,L}} \frac{1}{m} \sum_{t=1}^m (D_h(\mathbf{x}_{i_t}, \mathbf{x}_{j_t}) - y_t)^2. \quad (5)$$

90 We know from (4) in the main paper that $D_h(\mathbf{x}_i, \mathbf{x}_j) = b_i - b_j - \mathbf{a}_j^T(\mathbf{x}_i - \mathbf{x}_j)$, subject to the
 91 constraints given in Lemma 1 of the main paper. Therefore (5) can be solved as a quadratic program.

92 For the following generalization error bounds, we require that the training data be drawn iid. Note that
 93 while there are known methods to relax these assumptions, as shown for Mahalanobis metric learning
 94 in Bellet and Habrard [2], we assume here for simplicity that data is drawn iid¹ from $\mathcal{X} \times \mathcal{X} \times \mathcal{Y}$
 95 (and analogously for the relative distance case) with distribution μ . Each instance, $t \in [m]$, is a triple,
 96 $(\mathbf{x}_{i_t}, \mathbf{x}_{j_t}, y_t)$ drawn iid from μ .

97 We have the following result:

98 **Theorem 1.** Consider $S_m = \{(\mathbf{x}_{i_t}, \mathbf{x}_{j_t}, y_t), t \in [m]\} \sim \mu^m$. Let $\|\cdot\|_{\mu}^2 = \mathbb{E}[\|\cdot\|^2]$ and assume,

99 **A₁:** $\|\mathbf{x}\|_{\infty} \leq R$ and $\sup |y_t - \mathbb{E}[y_t | \mathbf{x}_{i_t}, \mathbf{x}_{j_t}]| \leq \sigma$, i.e. both the input and noise are bounded.

¹In many cases this is justified. For instance, in estimating quality scores for items, one often has data corresponding to item-item comparisons [8]; for each item, the learner also observes contextual information. The feedback, y_t depends only on the pair $(\mathbf{x}_{i_t}, \mathbf{x}_{j_t})$, and as such is independent of other comparisons.

100 **A₂**: $E[y_i | \mathbf{x}_{i_t}, \mathbf{x}_{j_t}] = D_\phi(\mathbf{x}_{i_t}, \mathbf{x}_{j_t})$, for a L -Lipschitz β -smooth function ϕ .

101 The generalization error of the empirical risk minimizer D_{h_m} of the regression loss on S_m ,

$$\begin{aligned} \|D_{h_m} - y_t\|_\mu^2 &\leq \|D_{h_m} - y_t\|_{S_m}^2 \\ &\quad + 16MKLR\sqrt{2\ln(2d+2)/m} \\ &\quad + M^2\sqrt{\ln(1/\delta)/(2m)}, \end{aligned}$$

102 with probability at least $1 - \delta$. Furthermore, D_{h_m} converges to the ground truth Bregman divergence
103 D_ϕ and the approximation error is bounded by

$$\begin{aligned} \|D_{h_m} - D_\phi\|_\mu^2 &\leq 36^2\beta^2R^4K^{-\frac{2}{d}} \\ &\quad + 16MKLR\sqrt{2\ln(2d+2)/m} \\ &\quad + M^2\sqrt{2\ln(2/\delta)/m}, \end{aligned}$$

104 where $M = 4LR + \sigma$. By choosing $K = \lceil m^{\frac{d}{4+2d}} \rceil$ we get: $\|D_{h_m} - D_\phi\|_\mu^2 = \mathcal{O}_p(m^{-\frac{1}{d+2}})$.

105 Consider $S_m \sim \mu^m$ be a set of m i.i.d data points. If $|f(\mathbf{x}) - y| \leq M$ for all $f \in \mathcal{F}$, \mathbf{x} and y , by a
106 standard Rademacher generalization result:

$$\|f(\mathbf{x}) - y\|_\mu^2 \leq \|f(\mathbf{x}) - y\|_{S_m}^2 + 2MR_m(\mathcal{F}) + M^2\sqrt{\frac{\ln 1/\delta}{2m}},$$

107 with probability greater than $1 - \delta$. By substituting $f = D_{h_m}$, and $\mathcal{F} = \mathcal{D}_{P,L}$ in the above we
108 immediately get the first line of the proposition.

109 Further for the empirical risk minimizer f_m we have that for all $\hat{f} \in \mathcal{F}$ that doesn't depend on the
110 training data S_m :

$$\begin{aligned} \|f_m(\mathbf{x}) - f_*(\mathbf{x})\|_\mu^2 &\leq \|\hat{f}(\mathbf{x}) - f_*(\mathbf{x})\|_\mu^2 + 2MR_m(\mathcal{F}) \\ &\quad + 2M^2\sqrt{(\ln 2/\delta)/(2m)}, \end{aligned} \tag{6}$$

111 where f_* is $\mathbb{E}[y|\mathbf{x}]$. This comes from the fact that during training f_m was chosen and not \hat{f} . By
112 substituting $f_m = D_{h_m}$, $f_* = D_\phi$, $\hat{f} = D_h = \arg \inf_{h \in \mathcal{F}_{P,L}} \|D_\phi - D_h\|_\infty$ and $\mathcal{F} = \mathcal{D}_{P,L}$ in (6)
113 we have:

$$\begin{aligned} \|D_{h_m} - D_\phi\|_\mu^2 &\leq \|D_h - D_\phi\|_\mu^2 + 2MR_m(\mathcal{D}_{P,L}) \\ &\quad + 2M^2\sqrt{(\ln 2/\delta)/(2m)} \\ &\leq \|D_h - D_\phi\|_\infty^2 + 2MR_m(\mathcal{D}_{P,L}) \\ &\quad + 2M^2\sqrt{(\ln 2/\delta)/(2m)} \\ &\stackrel{Thm1}{\leq} (36R^2\beta K^{-\frac{1}{d}})^2 + 2MR_m(\mathcal{D}_{P,L}) \\ &\quad + 2M^2\sqrt{(\ln 2/\delta)/(2m)}. \end{aligned}$$

114 Now by substituting $M = 4LR + \sigma$ and $R_m(\mathcal{D}_{P,L})$ from the value given by Lemma 2 we get the
115 proposition. The only thing left to prove is to show $\forall h \in \mathcal{F}_{P,L}$ and $\forall(\mathbf{x}, \mathbf{x}', y)$; the error is bounded,
116 i.e. $|y - D_h(\mathbf{x}, \mathbf{x}')| \leq M = 4LR + \sigma$:

$$\begin{aligned} |y - D_h| &\leq |D_h - \mathbb{E}[y|\mathbf{x}, \mathbf{x}']| + |y - \mathbb{E}[y|\mathbf{x}, \mathbf{x}']| \\ &\leq |D_h - D_\phi| + \sigma \\ &\leq \max\{|D_h|, |D_\phi|\} + \sigma \\ &= |\phi(\mathbf{x}) - \phi(\mathbf{x}') - \nabla\phi(\mathbf{x}')^T(\mathbf{x} - \mathbf{x}')| + \sigma \\ &\leq 2\|\nabla\phi(\mathbf{x}')\|_1\|\mathbf{x} - \mathbf{x}'\|_\infty + \sigma = 4LR + \sigma. \end{aligned}$$

117 **A6 Farthest-point clustering and $K < n$**

118 The algorithm given in the paper assumes that the number of hyperplanes K is equal to n ; this is
119 mainly for simplicity of presentation. In practice we often want to have $K < n$. Here we discuss
120 details of this approach, which we utilize in our experiments.

121 We apply a farthest-point clustering to the data first into K clusters, and then fix the assignments
 122 of points to hyperplanes using this clustering. With this assignment in place, we can then apply a
 123 minor modification to the PBDL algorithm to approximate the Bregman divergence. Farthest-point
 124 clustering is a simple greedy algorithm for a K-center problem, where the objective is to divide the
 125 space into K partitions such that the farthest distance between a data point and its closest partition
 126 center μ_i is minimized. This problem can be formulated as: given a set of n points x_1, \dots, x_n a
 127 distance metric $\|\cdot\|$ and a predefined partition size K , find a partition of data C_1, \dots, C_k and partition
 128 centers μ_1, \dots, μ_K to minimize the maximum radius of the clusters:

$$\max_i \max_{x \in C_i} \|x - \mu_i\|.$$

129 The farthest point clustering introduced in [5] initially picks a random point x_{0_0} as the center of
 130 the first cluster and adds it to the center set C . Then for iterations $t = 2$ to k does the following:
 131 at iteration t , computes the distance of all points from the center set $d(x, C) = \min_{\mu \in C} \|x - \mu\|$.
 132 Add the point that has the largest distance from the center set (say x_{t_0}) to the center set. Report
 133 x_{0_0}, \dots, x_{K_0} as the partition centers and assign each data point to its closest center.

134 Authors of [5] proved that farthest-point clustering is a 2-approximation algorithm (i.e. , it computes
 135 a partition with maximum radius at most twice the optimum) for any metric. Therefore there is
 136 a relation between the partition found by farthest-point clustering and covering set. Assume a set
 137 $\{x_1, \dots, x_n\} \subset \Omega$ has a ϵ -cover of size K over a metric $\|\cdot\|$. The partition found by farthest point
 138 clustering of size K is a 2ϵ -cover for $\{x_1, \dots, x_n\}$.

139 A7 Parameterizing Bregman divergences by piecewise linear functions

140 We parameterize the Bregman divergence using max-affine functions $h(x) = \max_{k=1, \dots, K} a_k^T x + b_k$.
 141 Using Lemma 1 from our paper with a predefined partition of the training data points x_1, \dots, x_n
 142 to $C = \{C_1, \dots, C_K\}$ and defining the mapping $p_i \doteq k$ given $x_i \in C_k$, we can write any pairwise
 143 divergence on training set as

$$\begin{aligned} D_h(x_i, x_j) &= h(x_i) - h(x_j) - \nabla h(x_j)^T (x_i - x_j) \\ &= (a_{p_i}^T x_i + b_{p_i}) - (a_{p_j}^T x_j + b_{p_j}) - a_{p_j}^T (x_i - x_j) \\ &= b_{p_i} - b_{p_j} + (a_{p_i} - a_{p_j})^T x_i, \end{aligned}$$

144 which is linear in terms of the parameters $a_k, b_k, k = 1, \dots, K$. Therefore if the loss function

$$\mathcal{L}(\phi) = \sum_{i=1}^m c_i (D_\phi, X, y) + \lambda r(\phi),$$

145 is a convex function of pairwise divergences, it will be a convex loss in terms of parameters. Further-
 146 more one needs to satisfy the constraints given by Lemma 1 in our paper to make sure $h(x)$ remains
 147 convex, i.e:

$$b_{p_j} + a_{p_j}^T x_j \geq b_k + a_k^T x_j, \quad j = 1, \dots, n, \quad k = 1, \dots, K,$$

148 which are linear inequality constraints. Therefore one can minimize the loss $\mathcal{L}(\phi)$ as a convex
 149 optimization problem.

150 A8 Additional Experimental Results

151 Bregman divergence regression on synthetic data

152 In this section, we experiment with regression tasks on synthetic data. In particular, we show that if
 153 data arises from a particular Bregman divergence, our method can discover the underlying divergence
 154 whereas Mahalanobis metric learning methods cannot.

155 **Data:** We generate 100 synthetic data points in three ways: i) discrete probability distributions
 156 $\{(p_1, p_2)\} | p_1 + p_2 = 1, p_1, p_2 \geq 0\}$ sampled from a Dirichlet probability distribution $Dir([1]_{1 \times 2})$,
 157 with a target value y computed as the KL divergence between pairs of distributions; ii) symmetric
 158 2-2 matrices sampled from a Wishart distribution $W_2([1]_{1 \times 2}, 10)$ with target value y computed
 159 as the $LogDet$ divergence between pairs; iii) data points are sampled uniformly from a unit-ball
 160 $\mathcal{B}([0.6]_{1 \times 2}, 1)$ with target value y computed as the *Itakura-Saito* distance between pairs; iv) data
 161 points are sampled uniformly from a unit-ball $\mathcal{B}([0.6]_{1 \times 2}, 1)$ with target value y computed as the

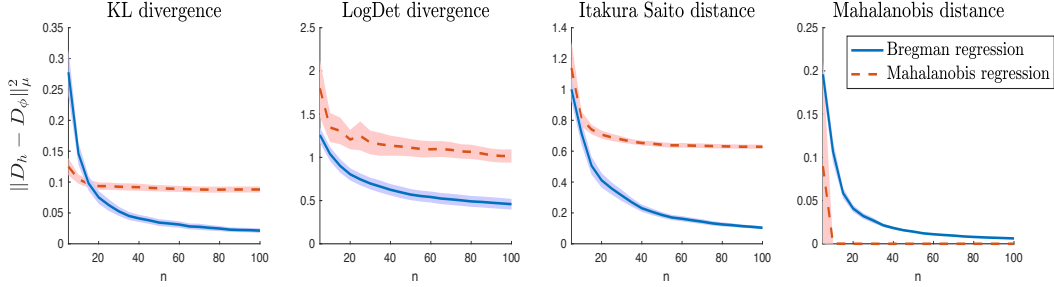


Figure 3: Regression with data from various Bregman divergences using PBDL and linear metric learning.

162 *Mahalanobis* distance between pairs. In each case we add Gaussian noise with stdev 0.05 to the ground
 163 truth divergences. For training, we provide all pairs of an increasing set of points ($\{(\mathbf{x}_i, \mathbf{x}_j), y_{i,j}\}$
 164 for (i, j) in the power set of $\{\mathbf{x}_1, \dots, \mathbf{x}_m\}$) and the target values y_i as noisy Bregman divergence of
 165 those pairs. For testing, we generate 1000 data points from the same distribution and use noiseless
 166 Bregman divergences as targets. Results are averaged over 50 runs.

167 **Details and observations:** For Bregman regression, we choose the Lipschitz constraint of PBDL for
 168 regression to be ∞ since the result was not sensitive to the choice of L . For *Mahalanobis regression*
 169 we do gradient descent for optimizing the least-square fit of a general Mahalanobis metric with the
 170 observed data which is done until convergence (as the problem is convex). We see from Figure 2
 171 that Mahalanobis metric learning is not flexible enough to model the data coming from the first three
 172 divergences, whereas the proposed divergence learning framework *PBDL* is shown to drastically
 173 improve the fit and seems to be a consistent estimator as motivated earlier in Theorem 1.

174 Nearest neighbor classification and additional data sets

175 We also present results on nearest neighbor classification and more data sets. Table 2 gives some
 176 additional performance numbers; in particular, we have added two new data sets and shown results of
 177 k-nearest neighbor classification.

Table 1: Learning Bregman divergences (PDBL) compared to existing linear and non-linear metric learning approaches on standard UCI benchmarks. PDBL performs first or second among these benchmarks in 22 of 30 comparisons, outperforming all of the other methods. Note that the top two results for each setting are indicated in bold.

Data-set	Algorithm	Clustering		Ranking		KNN ACC
		Rand-Ind %	Purity %	AUC %	Ave-P %	
Iris	PBDL	94.5 ± 0.8	95.6 ± 0.7	96.5 ± 0.4	93.5 ± 0.7	95.3 ± 0.7
	ITML [3]	96.4 ± 0.8	97.0 ± 0.7	97.5 ± 0.3	95.3 ± 0.5	97.4 ± 0.6
	LMNN [10]	90.0 ± 1.3	91.0 ± 1.3	94.3 ± 0.6	89.9 ± 0.8	96.1 ± 0.6
	GB-LMNN [7]	88.7 ± 1.5	89.9 ± 1.5	94.0 ± 0.6	89.7 ± 0.8	95.6 ± 0.6
	GMML [11]	93.8 ± 0.9	94.5 ± 0.9	95.7 ± 0.4	92.0 ± 0.6	96.6 ± 0.5
	Kernel NCA [4]	89.9 ± 1.3	90.3 ± 1.1	93.4 ± 0.6	88.3 ± 0.9	91.8 ± 1.4
Ionosphere	PBDL	65.2 ± 1.9	77.2 ± 1.9	65.8 ± 0.8	71.1 ± 0.8	81.4 ± 1.0
	ITML	72.2 ± 1.5	83.3 ± 1.2	71.5 ± 0.7	74.6 ± 0.6	85.0 ± 1.0
	LMNN	58.3 ± 1.2	70.8 ± 1.2	62.2 ± 1.3	69.8 ± 0.9	87.1 ± 0.8
	GB-LMNN	58.5 ± 0.9	70.9 ± 1.0	64.4 ± 1.3	71.2 ± 1.0	88.3 ± 0.9
	GMML	61.7 ± 1.8	73.9 ± 1.7	66.3 ± 0.8	71.3 ± 0.6	82.3 ± 1.0
	Kernel NCA	65.4 ± 1.7	77.7 ± 1.5	68.8 ± 1.1	72.0 ± 0.9	84.3 ± 1.0
Balance Scale	PBDL	84.4 ± 0.7	87.8 ± 0.5	86.0 ± 0.4	82.9 ± 0.5	91.4 ± 0.4
	ITML	68.9 ± 0.9	77.5 ± 0.7	80.1 ± 0.7	74.3 ± 0.8	90.0 ± 0.6
	LMNN	69.5 ± 1.8	77.0 ± 1.7	75.9 ± 1.3	70.0 ± 1.2	87.4 ± 0.5
	GB-LMNN	71.4 ± 1.5	79.7 ± 1.4	78.1 ± 1.1	72.2 ± 1.0	87.8 ± 0.6
	GMML	72.9 ± 0.8	80.2 ± 0.8	79.0 ± 0.4	72.8 ± 0.5	87.2 ± 0.6
	Kernel NCA	65.3 ± 1.5	73.0 ± 1.6	68.7 ± 1.8	63.7 ± 1.9	79.9 ± 1.7
Wine	PBDL	83.7 ± 2.9	85.0 ± 3.2	91.0 ± 0.9	86.7 ± 1.2	94.3 ± 0.9
	ITML	82.8 ± 2.6	82.5 ± 3.1	89.1 ± 1.1	84.6 ± 1.4	93.8 ± 1.0
	LMNN	70.0 ± 0.8	68.8 ± 1.2	82.4 ± 0.8	76.2 ± 1.1	91.7 ± 0.8
	GB-LMNN	70.6 ± 0.9	69.3 ± 1.4	83.7 ± 0.1	78.5 ± 1.3	93.8 ± 0.8
	GMML	83.2 ± 2.9	81.0 ± 3.2	91.0 ± 0.7	88.5 ± 0.7	96.5 ± 0.8
	Kernel NCA	70.4 ± 1.3	71.3 ± 1.4	75.1 ± 0.9	67.7 ± 1.1	67.5 ± 1.2
Transfusion	PBDL	57.9 ± 1.2	75.9 ± 0.7	54.9 ± 0.4	68.2 ± 0.6	75.7 ± 0.7_s
	ITML	60.2 ± 1.0	75.8 ± 0.7	54.2 ± 0.4	66.4 ± 0.7	74.5 ± 0.6
	LMNN	59.4 ± 1.3	76.3 ± 0.6	54.0 ± 0.5	67.1 ± 0.7	75.0 ± 0.7
	GB-LMNN	58.9 ± 1.2	76.3 ± 0.6	54.8 ± 0.6	67.2 ± 0.7	74.1 ± 0.7
	GMML	59.3 ± 1.3	76.6 ± 0.7	54.0 ± 0.5	67.5 ± 0.7	76.1 ± 0.6
	Kernel NCA	63.7 ± 0.7	76.2 ± 0.7	52.2 ± 0.8	65.7 ± 0.8	74.7 ± 0.8
Figure 1 data	PBDL	98.2 ± 0.3	98.6 ± 0.2	97.3 ± 0.3	95.6 ± 0.5	99.1 ± 0.2
	ITML	76.2 ± 1.6	74.9 ± 2.5	90.5 ± 0.5	83.7 ± 0.5	99.0 ± 0.2
	LMNN	73.4 ± 1.7	69.3 ± 2.6	90.4 ± 0.7	83.2 ± 0.7	98.8 ± 0.2
	GB-LMNN	73.3 ± .5	71.3 ± 2.6	90.5 ± 0.8	83.4 ± 1.0	99.2 ± 0.2
	GMML	73.9 ± 1.8	70.8 ± 2.8	91.4 ± 0.2	84.2 ± 0.3	98.9 ± 0.2
	Kernel NCA	76.5 ± 2.4	73.9 ± 3.7	90.4 ± 0.6	83.9 ± 0.6	98.0 ± 0.5

178 **References**

- 179 [1] Anthony, M. and Bartlett, P. L. (2009). *Neural network learning: Theoretical foundations.*
180 cambridge university press.
- 181 [2] Bellet, A. and Habrard, A. (2015). Robustness and generalization for metric learning. *Neurocom-*
182 *puting*, 151:259–267.
- 183 [3] Davis, J. V., Kulis, B., Jain, P., Sra, S., and Dhillon, I. S. (2007). Information-theoretic metric
184 learning. In *Proceedings of the 24th international conference on Machine learning*, pages 209–216.
185 ACM.
- 186 [4] Goldberger, J., Hinton, G. E., Roweis, S. T., and Salakhutdinov, R. R. (2005). Neighbourhood
187 components analysis. In *Advances in neural information processing systems*, pages 513–520.
- 188 [5] Gonzalez, T. F. (1985). Clustering to minimize the maximum intercluster distance. *Theoretical*
189 *Computer Science*, 38:293–306.
- 190 [6] Hölder, O. (1889). Ueber einen mittelwerthabsatz. *Nachrichten von der Königl. Gesellschaft der*
191 *Wissenschaften und der Georg-Augusts-Universität zu Göttingen*, 1889:38–47.
- 192 [7] Kedem, D., Tyree, S., Sha, F., Lanckriet, G. R., and Weinberger, K. Q. (2012). Non-linear metric
193 learning. In *Advances in neural information processing systems*, pages 2573–2581.
- 194 [8] Shah, N. B., Balakrishnan, S., Bradley, J., Parekh, A., Ramch, K., ran, and Wainwright, M. J.
195 (2016). Estimation from pairwise comparisons: Sharp minimax bounds with topology dependence.
196 *Journal of Machine Learning Research*, 17(58):1–47.
- 197 [9] Shalev-Shwartz, S. and Ben-David, S. (2014). *Understanding machine learning: From theory to*
198 *algorithms*. Cambridge university press.
- 199 [10] Weinberger, K. Q. and Saul, L. K. (2009). Distance metric learning for large margin nearest
200 neighbor classification. *Journal of Machine Learning Research*, 10(Feb):207–244.
- 201 [11] Zadeh, P., Hosseini, R., and Sra, S. (2016). Geometric mean metric learning. In *International*
202 *conference on machine learning*, pages 2464–2471.